GLAST LAT SUBSYSTEM TECHNICAL DOCUMENT	Document # **LAT-TD-01872**	Date Effective 03/27/03
	Prepared by(s) Alex Moiseev	Supersedes None
	Subsystem/Office Anticoincidence Detector Subsystem	
Document Title ACD Backsplash Testing at CERN		

Gamma-ray Large Area Space Telescope (GLAST)
Large Area Telescope (LAT)

ACD Backsplash Testing at CERN

1. Purpose

This study reports the results of backsplash tests for the ACD using high-energy particle beams at CERN.

2. Definitions and Acronyms

ACD	The LAT Anti-Coincidence Detector Subsystem
ADC	Analog-to-Digital Converter
AEM	ACD Electronics Module
ASIC	Application Specific Integrated Circuits
BEA	Base Electronics Assembly
CAL	The LAT Calorimeter Subsystem
DAQ	Data Acquisition
EGSE	Electrical Ground Support Equipment
EMC	Electromagnetic Compatibility
EMI	Electromagnetic Interference
ESD	Electrostatic Discharge
FM	Flight Module
FMEA	Failure Mode Effect Analysis
FREE	Front End Electronics
GAFE	GLAST ACD Front End – Analog ASIC
GARC	GLAST ACD Readout Controller – Digital ASIC
GEVS	General Environmental Verification Specification
GLAST	Gamma-ray Large Area Space Telescope
HVBS	High Voltage Bias Supply
ICD	Interface Control Document
IDT	Instrument Development Team
I&T	Integration and Test
IRD	Interface Requirements Document
JSC	Johnson Space Center
LAT	Large Area Telescope
MGSE	Mechanical Ground Support Equipment
MLI	Multi-Layer Insulation
MPLS	Multi-purpose Lift Sling
PCB	Printed Circuit Board

PDR	Preliminary Design Review
PMT	Photomultiplier Tube
PVM	Performance Verification Matrix
QA	Quality Assurance
SCL	Spacecraft Command Language
SEL	Single Event Latch-up
SEU	Single Event Upset
SLAC	Stanford Linear Accelorator Center
TACK	Trigger Acknowledge
TDA	Tile Detector Assembly
T&DF	Trigger and Data Flow Subsystem (LAT)
TBD	To Be Determined
TBR	To Be Resolved
TSA	Tile Shell Assembly
TSS	Thermal Synthesizer System
TKR	The LAT Tracker Subsystem
VME	Versa Module Eurocard
WBS	Work Breakdown Structure
WOA	Work Order Authorization

3. Applicable Documents

Documents relevant to the ACD Photomultiplier Quality Plan include the following.

1. LAT-SS-00016, LAT ACD Subsystem Requirements – Level III Specification
2. LAT-SS-00352, LAT ACD Electronics Requirements – Level IV Specification
3. LAT-SS-00437, LAT ACD Mechanical Requirements – Level IV Specification
4. LAT-MD-00039-01, LAT Performance Assurance Implementation Plan (PAIP)
5. LAT-MD-00099-002, LAT EEE Parts Program Control Plan
6. LAT-SS-00107-1, LAT Mechanical Parts Plan
7. LAT-MD-00078-01, LAT System Safety Program Plan (SSPP)
8. ACD-QA-8001, ACD Quality Plan
9. LAT-TD-00760-D1 Selection of ACD Photomultiplier Tube

10. LAT-DS-00739-1 Specifications for ACD Photomultiplier Tubes
11. LAT-TD-00438-D2 LAT ACD Light Collection/Optical Performance Tests
12. LAT-TD-00720-D1 ACD Phototube Helium Sensitivity
13. LAT-DS-00740-1 Temperature Characteristics of ACD Photomultiplier Tubes
14. Response to RFQ 5-09742, Hamamatsu Photomultiplier Tube Proposal

Backsplash study at CERN in 2002

A. Moiseev on behalf of the team of R. Hartman, T. Johnson, T.Kamae, J. Mitchell, T. Mizuno, J. Ormes, S. Ritz, and D. Thompson

The goal of this beam test was to provide a detailed study of the backsplash effect. This effect is unavoidable at high energies for particle detecting instruments which have calorimeters. In particular in the current experiment we tested calorimeter simulators made of lead, tin, and iron, from 8 X_0 to 30 X_0 thick. The particle detector where the backsplash was measured was a LAT ACD prototype made of eight 1 cm thick plastic scintillator tiles with wave-length shifting fiber readout. The test setup is shown in fig.1. Tiles 2, 3, and 4 are 8cm by 24 cm in size, the remaining tiles are 6cm by 24cm.

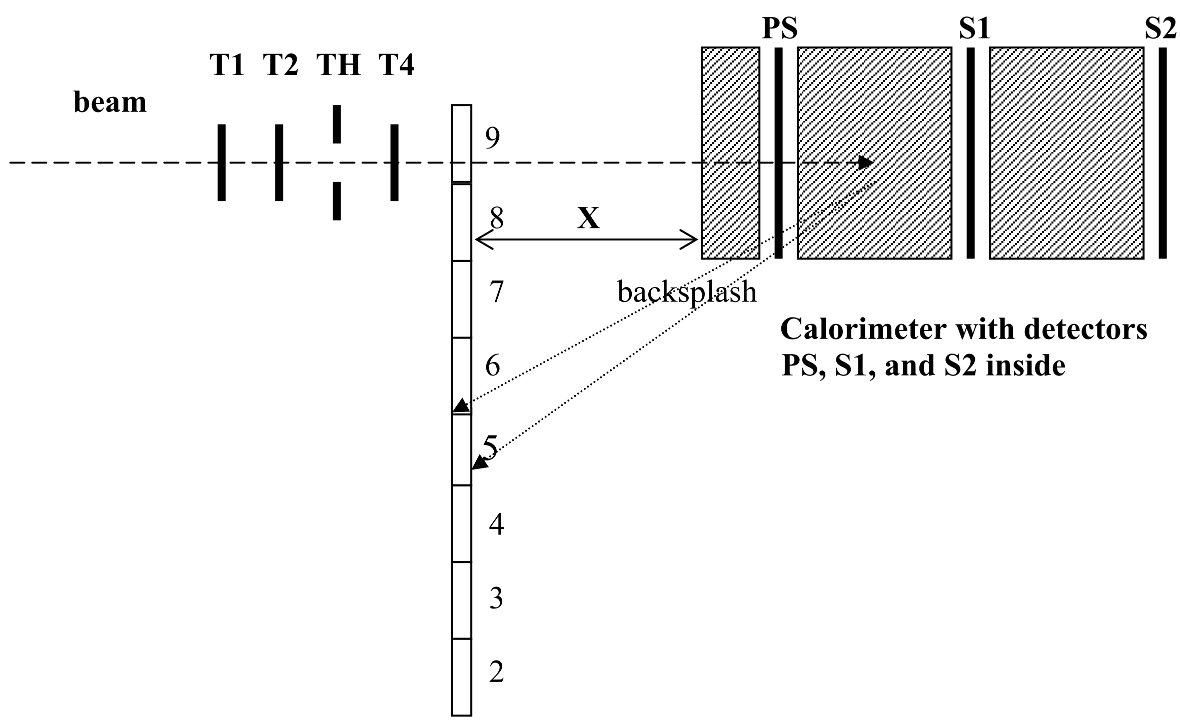

Fig.1 Experimental setup. ACD tiles are numbered from 2 to 9. T1, T2, TH, and T4 - triggering scintillators. PS, S1 and S2 - shower detectors, placed inside calorimeter. X - distance between ACD tiles and calorimeter front face.

The test took place on H4 beam line of CERN SPS in July, 2002. We were running electrons from 10 GeV to 250 GeV, and total number of data collection runs was 51. The data taking runs were preceded by the hard work of John Mitchell who adjusted and calibrated the electron beam. It took him almost 3 12-hours shifts to complete this challenging work. The next step of our measurements was to carefully measure the background which accompanies the electron beam (mainly bremsstrahlung photons with some secondary electrons). This background creates the same signals in the ACD as the backsplash effect being studied, so we have to know it to correct for it. Our previous CERN test data collected in 1999 lacked these data. The background measurements were performed without any calorimeter in the beam, so the detected spectrum in ACD tiles was assumed to be a background to the backsplash to be measured with the calorimeter present.

The subjects of the current test were the following:

- study incident particle energy dependence of the amount and spectrum of backsplash-caused signals in ACD tiles. Backsplash was produced in calorimeters made of lead, tin, and iron
- study the backsplash dependence on the distance between the ACD tiles and the calorimeter front face.
- study the backsplash dependence on the calorimeter material. Our predictions were that the backsplash amount depends on the calorimeter thickness in g/cm^2, not on the thickness in the radiation lengths X_0.

As a result of this work, a more exact formula for backsplash prediction has been found, and more precise backsplash predictions for LAT ACD have been made.

Experimental equipment.

Calorimeter simulator. We used metal plates of different thickness to imitate the calorimeters. Our earlier measurements and simulations hinted to us that the backsplash production depends on the atomic number Z of the material the calorimeter is made of. The tin (Z=50) plate is the best candidate to imitate the real CsI (Z=54) calorimeter. For the current beam test the following calorimeter simulators were available:

- 9.5 cm (7.9 X_0) of tin (Z=50) – simulator of LAT CsI calorimeter
- 14 cm (7.9 X_0) of iron (Z=26)
- 4.45 cm (7.9 X_0) of lead (Z=82)
- 9.5 cm (17 X_0) of lead
- 17.1 cm (30 X_0) of lead

ACD prototype was described above. It is basically the same unit which was built in 1997 for the beam test at SLAC that year, and later was exposed to the CERN beam in 1999.
The data readout was provided by CAMAC 2259 ADC and LabView software.
The triggering was provided by 3 scintillators in coincidence (T1 and T2 are 1 cm by 1 cm area, and T4 is 10cm by 10cm). The scintillator TH which was 10cm by 10cm with a1 cm diameter hole in the center was supposed to be used as VETO to reduce the charged background. But it appeared that the hole was too small to be reliably aligned with the beam in the conditions of the test, so we did not use this detector.

<u>The hadron contamination</u> was rejected by using shower detectors (scintillators) PS, S1, and S2, placed inside the calorimeter plates.
<u>The moving table</u> was built specifically for this test. It was remotely controlled and allowed us to scan the beam through the tiles and adjust its position without stopping the beam and entering the beam area.

<u>The data analysis procedure</u> was the following:

1. The response of every ACD tile to the MIP (minimum ionizing particle, here electron) was calibrated. To do this, we made 8 special runs, shooting the beam in the center of each ACD tile consecutively in each of these 8 runs. The MIP peak position was determined for each tile, and further the backsplash spectrum was measured in units of MIP for each tile.
2. For every run the set of events which interacted in the calorimeter was selected by applying the selections in the shower detectors PS, S1, and S2. Doing this we removed hadron contamination from the events to be analyzed. All further analysis steps were performed on this selected set of events.
3. For every run the spectrum of backsplash signals in each of the 8 ACD tiles was analyzed. The integral distribution was produced by calculating the number of events in the run with energy deposition in ACD tile to be more than 0.1, 0.2, 0.3, 0.4, and 0.5 MIP.
4. Background runs were treated similarly, and the measured background was subtracted from the corresponding spectrum bin in every run. The resulting spectrum was accepted as a backsplash-caused spectrum in ACD tiles.
5. In all results presented here unless stated differently, the backsplash is given in the fraction of events (in percent) in which the signal in ACD was above given threshold (in units of MIP). In most of figures the backsplash is given for tiles 6, 7, and 8 together with the total area of 432 cm^2.

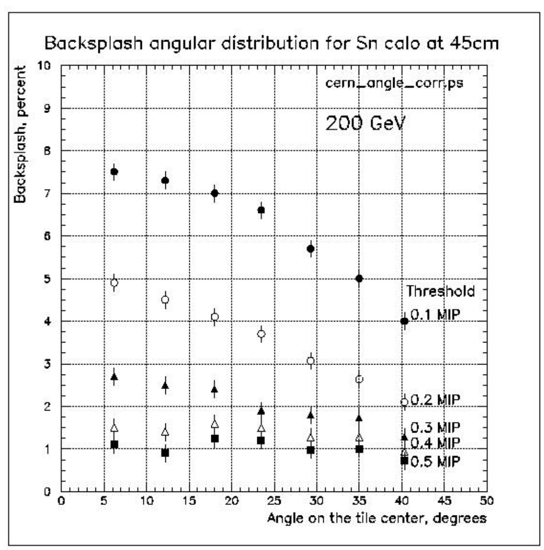

Fig.2 Angular distribution of backsplash

<u>Angular distribution of backsplash.</u>

This result is important for the LAT ACD backsplash prediction, because if the angular distribution would have sharp features, it would be more difficult to use approximations by propagating results obtained for smaller tiles to the larger tiles of LAT ACD. The angle under which the tile was seen from the calorimeter axis was measured between the beam axis and the line connecting the center of calorimeter face and the corresponding tile center. The results are given in fig.2 for all 5 signal thresholds used in the analysis. The area of tiles was 144 cm^2 (backsplash in larger tiles 2, 3, and 4 was scaled to the same area). The thresholds are in the units of MIP, which are different for every tile. These data are for 200 GeV beam, and taken for the tin calorimeter placed at 45 cm from the ACD plane. The size of top LAT ACD tile is given on the figure for comparison; it is seen that the backsplash within its size is acceptably uniform.

Energy dependence of backsplash.

In our previous studies we fitted the energy dependence of backsplash intensity by $E^{0.75}$. Our current measurements are given in fig.3 where the backsplash is given for tiles 6, 7, and 8 together (total area 432 cm^2) and for ACD tiles placed at 45 cm from the calorimeter face. Threshold used in this figure was 0.3 MIP. It is very easily seen how big the difference is in the backsplash intensity between the low Z (iron) and high Z (lead) calorimeters of the same thickness in radiation lengths. It is also seen that the backsplash

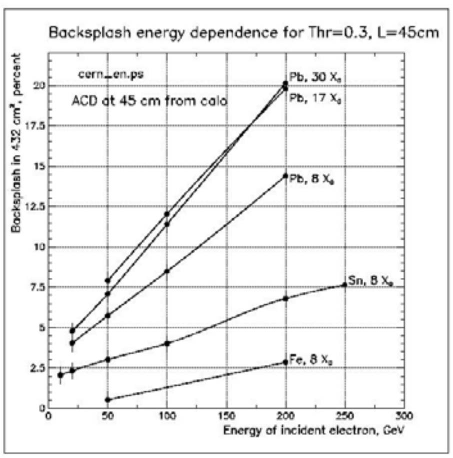

Fig.3 Measured energy dependence of backsplash for iron, tin, and lead calorimeters.

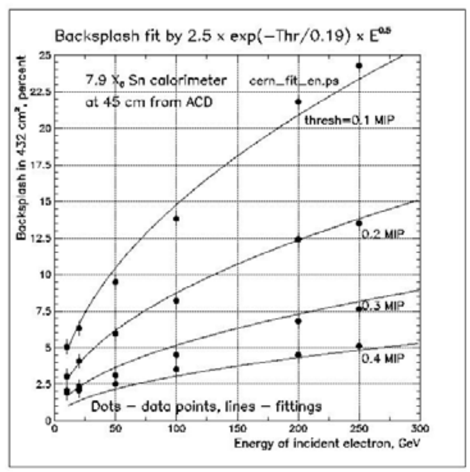

Fig.4 Fitting of backsplash energy dependence for tin calorimeter.

is significantly lower for $8X_0$ lead calorimeter than that for $17X_0$ and $30X_0$. But there is practically no difference between lead calorimeters of $17X_0$ and $30X_0$. This is because even for 200 GeV the shower maximum is at around $9X_0$, so the shower is completely contained within $17X_0$, and thickening of the calorimeter does not increase the backsplash.

Fig.4 shows the improved energy fitting for the tin calorimeter. The energy part of dependence is fitted by $E^{0.5}$, and the threshold dependence is fitted by exp(-Threshold/0.19), where Threshold is in the units of MIP. The average fitting precision of

~ 10% is achieved. We have to note that this fitting is usable only for this material (Sn or around on Z) and this thickness, appropriate for the LAT ACD.

Backsplash distance dependence.

For our previously developed backsplash formula we did not have the measurements made for different distances between the ACD tile and calorimeter front face. The measurements were done only for 45cm, and the predictions for LAT ACD design were made assuming common $1/r^2$ law. In LAT ACD all tiles, especially the side ones, are separated by different distances from the calorimeter, and better knowledge of distance effect is important.

In this test we measured the backsplash for 5 different distances using Sn calorimeter as the best imitator for real CsI calorimeter. The results are given in fig.5 where we attempted to compare the currently measured backsplash intensity with that predicted by our old formula. The data are given for energies 50 GeV and 200 GeV, along with the

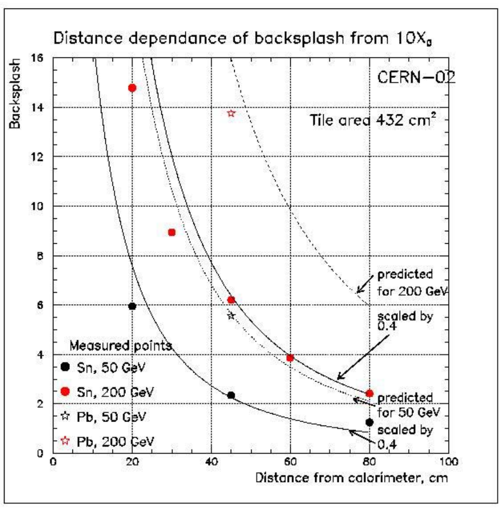

Fig.5. Distance dependence of backsplash for tin (circles) and lead (stars) calorimeters. Black points are for 50 GeV, red – for 200 GeV. Dashed lines – predictions by old formula, solid lines – the same predictions scaled by 0.4

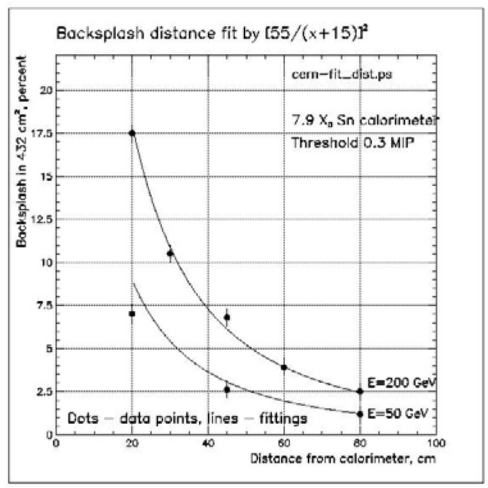

Fig.6 Fitting of the distance dependence for tin calorimeter. Filled circles – data points, lines – new fittings.

formula predictions (dashed lines). We see that if the previously-predicted backsplash is scaled by a factor of 0.4, it well agrees with the measured one for tin (filled circles, solid lines). Plotted data points for lead calorimeter (stars) also show good agreement with that predicted, of course without scaling. It confirms that our previously developed formula works well for a lead calorimeter and should be scaled down for lower Z calorimeters.

Fig.6 shows our improved fitting of distance dependence for the $7.9X_0$ tin calorimeter. The data points are given by filled circles for energies 50 GeV and 200 GeV, and the lines are the fittings by [55/(x+15)] where x is the distance between ACD and calorimeter front face in cm. Doing fitting we intentionally made it better for higher energy (200 GeV) because we need to know the backsplash better at the higher energy. For better fitting the term "15" which is related to the shower max position in the calorimeter should probably be energy dependent to reflect the shower development energy dependence. These fitting lines are made by our new backsplash formula

$$P_{backsplh} = 2.5 \times \exp\left(-\frac{E_{thr}}{0.19}\right) \times \frac{A}{432} \times \left(\frac{55}{x+15}\right)^2 \times \sqrt{E}$$

where $P_{backsplh}$ is the probability of backsplash (in percent) with threshold of E_{thr} measured in units of MIP, in the tile of area of A (in cm^2), for an ACD tile separated by x cm from the front face of calorimeter, and the incident electron (photon) energy of E [GeV]. This formula is valid for the 8-9 X_0 thick CsI (or made of material with close Z) calorimeter.

Calorimeter thickness dependence.

These measurements were performed for lead calorimeter of 3 thicknesses ($8X_0$, $17X_0$, and $30X_0$) and 4 energies (20, 50, 100, and 200 GeV). The results are given in fig.7. As has already been said above, the increase of backsplash with increasing thickness from 8 X_0 to $17X_0$ is clear, and the saturation of the backsplash (shower containment effect) for thicker calorimeters at these energies is also clear. It is unclear why the data points for $30X_0$ are lower that that for $17X_0$. We see this effect for all energies, which means different runs, so we cannot blame one particular run. One important thing can be concluded from these data – for finer correction for the exact calorimeter thickness around LAT thickness we should use the correction factor F of approximately

$$F = 1 + 0.07 \times (x - 7.9)$$

where x is the exact calorimeter thickness in radiation lengths. This formula is valid for thicknesses up to 13-14X_0 .

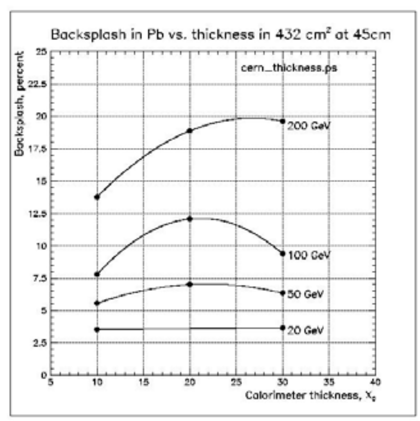

Fig.7 Backsplash thickness dependence for lead calorimeter

Calorimeter material dependence.

One of the things which was encountered in the simulations was that the backsplash intensity is mainly driven by the Z of the calorimeter material, or more exactly by the weight (in g/cm^2) of the material radiation length. Electromagnetic calorimeters of the same thickness in radiation length create less backsplash if they are made of material of lower Z, and consequently heavier X_0 in g/cm^2. It became clear because the backsplash is mainly soft photons which are absorbed by the grammage not by the radiation lengths. Fig.8 shows the results of current test (open circles for lead, tin, and iron calorimeters) compared with the simulation results obtained earlier. The difference between data and simulations has to be explored – very likely the simulations were made for not exactly the conditions of the experiment. Anyway, the trend confirms the conclusion about preferable calorimeter design, especially if heavy (in Z) calorimeter is not the best, for example the "cubic" version of hadronic calorimeter for ACCESS. The material dependence also resolves the concern about the difference between our previous test results in CERN'99 made with lead and tungsten calorimeters, and the LAT ACD simulations.

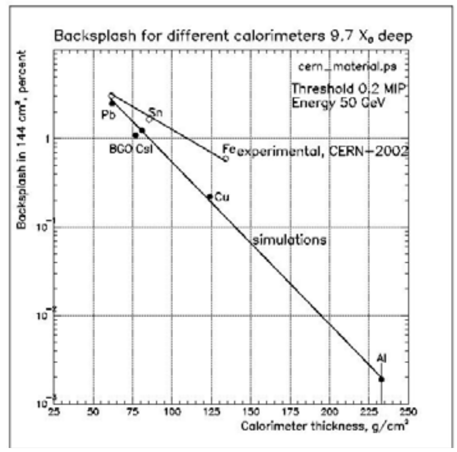

Fig.8 Backsplash material dependence. Open circles – current test results. Filled circles – earlier simulation data (to be checked!)

Predictions for LAT ACD.

The data obtained allow us to check the LAT ACD segmentation. The ACD was designed according to our old formula with the requirement not to have more than 20% of the events at 300 GeV to be self-vetoed by backsplash with the threshold of 0.3 of a MIP. This requirement is in strong conflict with the ACD efficiency requirement, and our current situation is that we have exhausted almost all our margins in the efficiency. The new backsplash prediction based on the current test is shown in fig.9. The energy was scaled to 300 GeV from the highest energy in the test of 250 GeV. The tile area was scaled as well. We can see that the results obtained for the lead calorimeter very well agree with our old formula prediction. The results for tin (read CsI) calorimeter demonstrate that the self-veto level will not be higher than 20% at threshold of 0.2 of the MIP. This gives us margins in the ACD efficiency performance. We need them because of

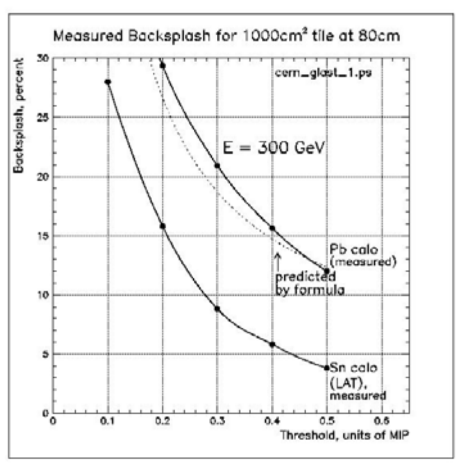

Fig.9 Backsplash predictions for LAT ACD top tile at 300 GeV

large light losses and large temperature performance variations. One more very important conclusion is that the use of ACD in level 1 Trigger will be more efficient because the use of "Nearest Neighbors" will have smaller effect on the efficiency. The threshold does not have to be low in Level 1 Trigger because the ACD does not have to have 0.9997 efficiency on this level.

Conclusions.

1. More reliable data were obtained with much better background rejection.
2. The measurements were done in a wide range of energy, ACD positions and calorimeter material, and calorimeter thickness. All that allowed us to improve the backsplash formula which can be used for quick simulation of LAT ACD performance.
3. The results obtained allowed us to count on more margin in ACD performance. This margin is not extremely critical to meet ACD requirements, but will make the future data analysis and mission operation easier.
4. The data obtained will allow us to validate the LAT ACD simulations, and also can contribute in validation of the simulation package as a whole.
5. The understanding of the material dependence can contribute in specific calorimeter design.

Acknowledgements

This whole work could not be completed without extremely valuable help by Deneen Ferro and Bill Daniels (detector fabrication and refurbishing) and Norm Dobson who developed the whole data acquisition system for this experiment. Special thanks to CERN SPS personnel whose help in the everyday work was great.